Thermal analysis of submicron nanocrystalline diamond films

S. Rossi[1], M. Alomari[1], Y. Zhang[2], S. Bychikhin[3], D. Pogany[3], J. M. R. Weaver[2], E. Kohn[1]

Authors affiliations:
[1]*Ulm University, Albert-Einstein-Allee 45, 89081 Ulm, Germany*
[2]*Department of Electronics and Electrical Engineering, University of Glasgow, Glasgow G12 8QQ, Scotland*
[3]*Institute for Solid-State Electronics, Vienna University of Technology, Floragasse 7, A-1040 Vienna, Austria*

Corresponding author:
S. Rossi (stefano.rossi@uni-ulm.de)
Ulm University
Albert-Einstein-Allee 45, Ulm 89081, Germany
Phone: +49 (0)731 5026183

Abstract

The thermal properties of sub-µm nanocrystalline diamond films in the range 0.37-1.1 µm grown by hot filament CVD, initiated by bias enhanced nucleation on a nm-thin Si-nucleation layer on various substrates, have been characterized by scanning thermal microscopy. After coalescence, the films have been outgrown with a columnar grain structure. The results indicate that even in the sub-µm range, the average thermal conductivity of these NCD films approaches 400 $Wm^{-1}K^{-1}$. By patterning the films into membranes and step-like mesas, the lateral and the vertical component of the thermal conductivity, $k_{lateral}$ and $k_{vertical}$, have been isolated showing an anisotropy between vertical conduction along the columns, with $k_{vertical} \approx 1000$ $Wm^{-1}K^{-1}$, and a weaker lateral conduction across the columns, with $k_{lateral} \approx 300$ $Wm^{-1}K^{-1}$.

1. Introduction

Diamond, in its single-crystalline form, has the highest room temperature thermal conductivity *k* of any known material, which reaches a value of 2200 $Wm^{-1}K^{-1}$ [1]. However, due to the difficulty of heteroepitaxial growth of single-crystalline diamond on foreign substrates, most applications utilize CVD-deposited poly-crystalline diamond films. The thermal properties of such films are strongly dependent on the microstructure [2], and *k* spans over two orders of magnitude, depending on the geometry of the grains and concentration of defects and impurities, which in turn are function of the growth process [3].

In general, the hetero-epitaxial growth of diamond begins by the nucleation of individual crystallites on the substrate. Microcrystalline diamond (MCD) films are outgrown in thermodynamic conditions which suppress re-nucleation phenomena and enhance competitive growth of the randomly oriented crystallites as they enlarge and merge, as modeled by van der Drift [4, 5]: the nuclei with their fastest growing orientation perpendicular to the surface will overgrow the slower facets as the film coalesces, so that a strong columnar texture develops in the film. In such a structure, the average in-plane dimensions of the grains increase with the distance *z* from the substrate according to the initial nucleation density and the alpha growth parameter [5, 6]. On the other hand, nanocrystalline diamond (NCD) films can be grown by allowing a little re-nucleation during the outgrowth, usually by using a very low concentration of methane in the growth process [7]. Thus, substantially thick NCD films can be grown, while maintaining the in-plane dimensions of the columns within hundreds of nanometers.

Scattering at the grain boundaries is the main phonon scattering mechanism [8, 9] in such polycrystalline material. The anisotropy in the shape of the grains, with an out-of-plane (i.e. vertical)

size much greater than the in-plane (i.e. lateral) size, should reflect in better heat conduction along the columns rather than across adjacent grains, which involve higher scattering rates. In addition, since the grains get larger with increasing distance from the substrate, and larger grain dimensions imply a lower concentration of grain boundaries, a gradient in thermal conductivity with film thickness is also expected.

Strong anisotropy and thickness-dependence in the thermal conductivity has indeed been reported by several studies on thick, columnar-structured MCD films [10, 11].
For instance, the results of Graebner et al. [8] indicate a strong dependence on the layer thickness for both components of k, with an anisotropy $k_{vertical}/k_{lateral} \approx 2$ (for thicknesses in the range of 30–100 μm) and values eventually reaching the natural diamond ones in both directions for film thicknesses above 200 μm. Evidence of strong thickness dependence of the thermal conductivity was observed also in thinner, columnar-structured NCD films by Philip et al. [7], who reported an increase in the thermal conductivity from 530 to 1370 $Wm^{-1}K^{-1}$, when the film thickness increased from 1.6 μm to 3.6 μm. On the one hand, these values demonstrate that columnar-NCD films can reach high thermal conductivities even in the μm range, with nearly 60% of the single crystal conductivity for 3.6 μm of material. However, on the other hand, these values do not carry information on the expected anisotropy between lateral and vertical thermal conductivity for the first stages of growth (the first hundreds of nanometers), which is a consequence of the anisotropic crystalline structure of these films.

The thermal characterization of such thin NCD films with high thermal conductivity represents a challenging task for both the heat generation and temperature detection methods employed for thin films characterization [12 and references within].
In fact, besides the high spatial (or temporal) resolution necessary to achieve a sufficient level of accuracy, those techniques using the thin film on a substrate approach (e.g. 3ω, laser-flash, thermo-reflectance methods) have to cope with heat conduction both by the NCD film and the substrate, a condition that makes the measurement and the interpretation of the results rather complicated. Moreover, an additional challenge is represented by the test structures when suspended bars, bridges or membranes need to be fabricated out of diamond films hundreds of nanometers thick.
Indeed, to the authors' best knowledge, only little information is available on the anisotropic thermal properties of NCD films in the submicron range of thicknesses [13, 14, 15].

The strategy followed in this work to address the challenges posed by the characterization of such thin films consist of: 1) controlling the heat fluxes in the NCD film by tailoring the geometry of the test structures; 2) adopting a temperature detection technique with nm-scale spatial resolution and 3) relying on thermal simulations to analyze the experimental data.
Reported here are the thermal properties of sub-μm thick NCD films grown with columnar structure, the microstructure of which is verified using atomic force microscopy (AFM) and scanning electron microscopy (SEM). The thermal properties of these films are investigated using a scanning thermal microscopy (SThM) method, applied on three sets of specifically designed test structures with different film thicknesses and different substrates, thus enabling the study of both the thickness-dependence and the anisotropy in the thermal conductivity. The lateral and vertical thermal conductivities of the film ($k_{lateral}$ and $k_{vertical}$) are quantified using finite element analysis (FEA) of the experimental data.

2. Experimental

The investigated NCD films were nucleated by BEN, using 100 nm PECVD-SiO_2/50 nm α-Si as a nucleation interlayer, and grown stepwise to several thicknesses on sapphire and Si substrates in a custom hot filament CVD reactor at 750 °C with 0.4% CH_4 diluted in H_2. In such conditions the diamond growth follows a columnar growth-mode, resulting in a textured film with elongated grains along the out-of-plane direction (i.e. normal to the substrate) [16]. All samples used were grown under nominally identical conditions, and the different film thicknesses (summarized in Table 1) were obtained by varying the total growth time only. For each sample, the average in-plane grain size at the surface was calculated from AFM maps, and the total film thickness was measured using SEM.

Three sets of structures (see Fig. 1) were adopted for thermal analysis by SThM as the following.

To investigate the thermal conductivity gradient with thickness, a first set of samples (Set1) comprising NCD films of three different thicknesses (370, 600 and 650 nm) grown on 330 µm thick sapphire substrates was used. Heater devices consisting of 8 x 0.16 μm^2 NiCr resistors, 33 nm thick, with gold connecting pads, were fabricated on the surface of each sample (see Fig. 2.a). Such a heater design, where heater's length (*L)* is much larger than both the heater's width (*W*) and the diamond layer thickness *D* (*L*>>*D*>>*W*), was adopted to approximate the condition of a linear heat source [17]. This condition, in addition to the high thermal impedance represented by the SiO_2/a-Si interlayer stack ($R_{interlayer} \approx 10^{-7}$ m^2KW^{-1} for $k_{interlayer} \sim 1.38$ $Wm^{-1}K^{-1}$) plus the low thermally conductive sapphire substrate ($k_{sapph} \sim 34$ $Wm^{-1}K^{-1}$) results in limited heat flow toward the substrate, and hence enhances the lateral heat spreading in the NCD film.

To investigate the lateral component of the thermal conductivity ($k_{lateral}$), a second set of samples (Set2) was fabricated into membrane structures, as shown in Fig 1.b. NCD films (0.5 µm and 1.1 µm thick) were grown on silicon substrates (350 µm thick), followed by fabricating the NiCr resistor lines, using the linear heater design described above. The substrate was then dry etched by anisotropic plasma etching (Bosch process, SF_6/C_4F_8) in an area of 100 x 200 μm^2 underneath the metal heaters, utilizing the diamond film as an etch-stop layer. In such a membrane structure, the heat generated by the metal heater located at the centre is constrained to flow laterally inside the diamond membrane, thus avoiding vertical losses through the substrate, and allowing the isolation of the lateral contribution of the thermal conductivity of the NCD film.

The vertical component of the thermal conductivity ($k_{vertical}$) was investigated using a third set of samples (Set3). NCD films 0.8 µm thick were grown on silicon and subsequently mesa-etched to the substrate by RIE in O_2 using the metal heaters fabricated on the surface as etch-mask. In the resulting MESA structure (see Fig. 1.c and 2.b) the NCD film is left only between the top metal heater and the substrate. Since the heat crosses the structured NCD film flowing in the direction parallel to the columnar grain structure, the heat losses due to lateral conduction are minimized. In this configuration, $k_{vertical}$ is estimated by measuring the temperature rise over the diamond step relative to the silicon substrate.

The thermal measurements on the three sample sets were conducted using the temperature-sensitive nano-probe of a Scanning Thermal Microscopy (SThM) measurement setup [18]. In addition to the high spatial resolution (~ 20 nm) and high temperature sensitivity (1 K) of this technique, the probe used in this work has been designed and fabricated to have reduced bending at high temperatures [18], thus providing accurate temperature maps of the sample for all the bias conditions of the heating devices. The samples were fixed by vacuum on the chuck of the SThM equipment, and DC-bias with power ≈ 15 mW was applied to the heater. Thermal scans were performed in air at standard conditions of pressure and temperature, with a scan rate of 0.2 Hz. In this configuration, the SThM chuck serves as heat-sink (at room temperature) for the heat generated by the heater on the top surface. The setup for thermal scanning and the custom-designed probe are described in details elsewhere [18, 19]. In order to obtain accurate temperature mapping of the sample surface, the probe was calibrated prior to every run of measurements using a microfabricated temperature standard based on a measurement of Johnson noise [19].

3. Results and discussion

Figure 3 shows the topographic and temperature maps obtained by SThM on sample *c* from Set1 (Set1_c). The temperature profile shown in Figure .a has been extracted from the temperature map by plotting the temperature along a line perpendicular to the metal heater and passing through its centre, where the highest temperature is reached. The surface temperature decays departing from the heater centre, with maximum $\Delta T \approx 30$ K. The measured trend is strongly non-linear due to heat losses to the SThM probe, to the environment and to the substrate (when present).

To handle the complexity of the analysis, the surface temperature profiles of each sample were analyzed by means of 3D-FEA thermal modelling and the thermal conductivity components were extracted by fitting the experimental data with the simulated thermal profile.
The value of k minimizing the difference $\Delta T = T_{sim} - T_{exp}$ between simulated and experimental curves in close proximity to the heater (see Fig. 4.b), i.e. in the region in which the contribution of the diamond film to the heat conduction is dominant, was chosen as best-fit value.
The FEA software solves the three-dimensional steady state heat diffusion equation [17]:

$$-k\nabla^2 T(x,y,z) = Q(x,y,z) \qquad (1)$$

where k is the thermal conductivity, T is the temperature and Q is the applied power density expressed in W/m^3. It is worth noticing that no electro-thermal interaction has been taken into account in the model. In addition, the temperature dependence for the thermal parameters has been neglected, since at the low power levels used in the experiments the temperature gradients (ΔT) remain well below 100 K.
Another approximation was used specifically for Set1.
Here the gradient in thermal conductivity with thickness of the film was modelled by means of a multi-layer structure consisting of up to three layers, labelled L_1, L_2, and L_3: L_1, with thickness t_1 and conductivity k_1, was used to model the thinnest sample in the set (Set1_a); the stack of L_1 plus L_2, with thickness t_2-t_1 and conductivity k_2, was used for the second sample (Set1_b); finally, the stack of L_1, L_2 plus L_3, with thickness t_3-t_2 and conductivity k_3, was used for the thickest sample (Set1_c).

The values of thermal conductivity k obtained by fitting the experimental data with the simulated curves are listed in Table 1.
As can be seen from the extracted values of k, the results of the analysis on the samples from Set1 show a strong correlation between film thickness and thermal properties, with a steady increase in thermal conductivity (more precisely in its local, thickness-averaged value) as the film gets thicker, with larger grains, from 230 $Wm^{-1}K^{-1}$ at 370 nm (in-plane grain size of 77 nm), to 410 $Wm^{-1}K^{-1}$ for the 650 nm thick film (in-plane grain size of 124 nm).

The observed trend can be correlated to the films microstructure by means of Figure 5, where the in-plane grain size of the films used in this work is plotted against their thickness. In order to illustrate the development of the columnar structure beyond the sub-micron range, data of thicker films grown using the same growth conditions is also reported.
As the plot shows, after an initial phase of fast in-plane growth, characterized by a linear growth-gradient γ_1, at a film thickness of approximately 1 µm the rate with which the grains grow laterally start to reduce significantly due to re-nucleation phenomena. New grains that formed during the outgrowth compete with the ones that developed from the initial nuclei, such that in average the in-plane dimensions of the grains increase only slightly, with gradient γ_2, while the growth can continue freely along the out-of-plane direction. According to the linear model sketched in the figure, the average in-plain grain dimensions d at a certain thickness z can be expressed as $d(z)=d_0+\gamma z$, where d_0 is the initial grain size and γ is the grain size gradient with thickness, different for the two range of thicknesses ($\gamma = \gamma_1$ for $z<1$ µm, $\gamma = \gamma_2$ for $z>1$ µm).
Since larger grains imply lower densities of grain boundaries and since scattering at the grain boundaries is the main factor limiting the phonon diffusion length in the NCD layer, a similar linear correlation should exist between film thickness (and hence average in-plain grain dimensions) and the film's thermal conductivity.
In Figure 6, the plot of k values for Set1 against the film thickness shows indeed a good agreement with the expected linear model.

However, the thermal conductivity estimated in such a way is labelled as “effective”, since it is inherently influenced by NCD film's anisotropy and by substrate's role in the heat conduction, and therefore subject to change when the very same NCD film (i.e. the same microstructure) is deposited on a different material, rather than sapphire, or when different boundary conditions between film and substrate are established.

This assumption was verified by Set2 and Set3, which aimed at revealing the lateral and vertical components of the anisotropic NCD thermal conductivity by modifying the boundary conditions of the measurement.
In Set2, a boundary with high thermal resistance is created at the nucleation side of the NCD by removing the substrate. This condition forces a large lateral heat flux within the film, thus revealing the actual heat transport properties of the NCD film in the lateral direction.
In Set3, BEN is performed directly on a bare Si substrate (without any additional interlayer coating), hence creating a boundary of low thermal resistance between the NCD film and the Si substrate. In fact, besides allowing homogeneous high nucleation density of more than 10^{10} nuclei/cm^2, the BEN establishes a covalent bond between diamond nuclei and substrate that results in strong mechanical adhesion and enhanced thermal contact (with R_{TBR} as low as $4 \cdot 10^{-9}$ m^{2}KW^{-1} for diamond on Si from [2]). Leaving the NCD film only in the area underneath the heater forces a large vertical heat flux through the film that represents NCD vertical thermal conductivity.

As can be seen from the results reported in Table 1, the lateral component of *k* strongly depends on the in-plane grain dimensions, with a 60% increase in $k_{lateral}$ in response to an increase of in-plane grain size from 110 to 188 nm. In addition, the lateral component is significantly lower than the vertical in the whole range of grain size explored in this study, with $k_{vertical}$ approaching 1000 Wm^{-1}K^{-1}, a value more than two times higher than $k_{lateral}$.
These results indicate that in the columnar-structured NCD films used in this investigation the heat flows predominantly in the vertical direction along the grains, rather than laterally across adjacent grains. This agrees well with the dirty-grain boundaries model describing the heat transport in the nanodiamond film. In fact, assuming that defects, impurities and dislocations responsible of phonon scattering are preferentially located at the grain boundaries, phonons diffusing vertically (and hence within the same grain) encounter significantly less scattering compared to phonons crossing the grain boundaries to diffuse laterally through several grains.

A comprehensive overview of the results can be gained from Figure 6, where the thermal conductivity values of the three sets are plotted as a function of film thickness.
Trend lines have been indicated in the graph according to a simplistic linear model, under the assumption that as the NCD thickness approaches zero, its thermal conductivity becomes comparable to the one of an amorphous material ($k \sim 1$ Wm^{-1}K^{-1} [20]) in both lateral and vertical direction.
In the first tens of nanometers, the NCD film has a disordered microstructure consisting of non-diamond, amorphous phases inter-mixed with diamond nanocrystals [1], similar to ultra-nanocrystalline diamond films, whose thermal conductivity is indeed rather low and isotropic (< 10 Wm^{-1}K^{-1} [21]).

The graph shows that even if the vertical thermal conductivity of columnar NCD films is ~400 Wm^{-1}K^{-1} at 300 nm and increases steadily with thickness, reaching 1000 Wm^{-1}K^{-1} already in the sub-µm range, the effective thermal conductivity may be significantly lower. For instance, a 500 nm thick NCD film has a $k_{effective} \approx k_{lateral} \sim 300$ Wm^{-1}K^{-1} when grown on sapphire, since the heat diffuses mainly laterally. Instead it may approach 650 Wm^{-1}K^{-1} when deposited on a high thermally conductive substrate, with low interface thermal resistance, conditions which allow better vertical heat conduction. Indeed thermal scans on a group of heater devices on a sample from Set2 where the Si substrate have not been etched away, led to $k_{effective} = 602$ Wm^{-1}K^{-1} against a value of 276 Wm^{-1}K^{-1} obtained for the membrane-structured film on the same sample.

4. Conclusions

In this study, NCD films outgrown in a columnar way up to ~1 µm and heated by resistive top heaters have been analysed by SThM by means of a novel thermo-sensitive probe mapping the surface temperature distribution. Test structures have been specifically designed and fabricated in order to extract relevant information on the thermal conductivity anisotropy of the films and correlate it with their microstructure. The study shows that such NCD films are indeed heterogeneous, with a clear dependence of the thermal conductivity *k* on the film's in-plane grain size and on the boundary

conditions in which the measurement is performed, such that care has to be taken in the interpretation of the extracted values. The results indicate that with a $k_{effective}$ > 300 $Wm^{-1}K^{-1}$ already in the sub-µm range, columnar NCD films approach the thermal conductivity of high thermally conductive materials like SiC (~300 $Wm^{-1}K^{-1}$ at RT [22]) or AlN (~270 $Wm^{-1}K^{-1}$ at RT [23]). They also indicate that these films can spread the heat more efficiently by vertical conduction along the columns (with $k_{vertical}$~1000 $Wm^{-1}K^{-1}$) than laterally across them ($k_{lateral}$~300 $Wm^{-1}K^{-1}$). Thus, in order to grow thin NCD films with high thermal conductivity, it is crucial to use growth parameters promoting the earliest development of large grains in the shortest distance from the substrate.

Acknowledgments: The research leading to these results has been funded by the Seventh Framework Programme FP7/2007-2011 under grant agreement n°214610, project MORGaN.

References

[1] G. A. Slack, Thermal Conductivity of Pure and Impure Silicon, Silicon Carbide, and Diamond, J. Appl. Phys. 35, (1964) 3460–3466.
[2] H. Verhoeven, A. Floter, H. Reib, R. Zachai, D. Wittorf, and W. Jager, Influence of the Microstructure on the Thermal Properties of Thin Polycrystalline Diamond Films, Appl. Phys. Lett. 71 (1997) 1329.
[3] J. E. Graebner, H. Altmann, N. M. Balzaretti, R. Campbell, H. Chae, A. Degiovanni, R. Enck, A. Feldman, D. Fournier, J. Fricke, J. S. Goela, K. J. Gray, Y. Q. Gu, I. Hatta, T. M. Hartnett, R. E. Imhof, R. Kato, P. Koidl, P. K. Kuo, T. Lee, D. Maillet, B. Remy, J. P. Roger, D. Seong, R. P. Tye, H. Verhoeven, E. Wo, J. E. Yehoda, R. Zachai, and B. Zhang, Report on a second round robin measurement of the thermal conductivity of CVD diamond, Diamond and Related Materials 7 (1998) 1589–1604.
[4] A. van der Drift, Philips Research Report 22 (1967) 267.
[5] C. Wild, N. Herres, P. Koidl, J. Appl. Phys. 68 (1990) 973.
[6] C. Wild, P. Koidl, W. Mullersebert, H. Walcher, R. Kohl, N. Herres, R. Locher, R. Samlenski, R. Brenn, Diamond and Related Materials 2 (1993) 158.
[7] J. Philip, P. Hess, T. Feygelson, J. E. Butler, S. Chattopadhyay, K. H. Chen, and L. C. Chen, Elastic, mechanical, and thermal properties of nanocrystalline diamond films, J. Appl. Phys. 93 (2003) 2164–2171.
[8] K.E. Goodson, O.W. Käding, and R. Zachai, ASME HTD Proceedings, 292 (1994) 83.
[9] K.E. Goodson, ASME/JSME Thermal Engineering Conference, 4 (1995) 183.
[10] J. E. Graebner, S. Jin, G. W. Kammlott, J. A. Herb, and C. F. Gardinier, Unusually high thermal conductivity in diamond films, Appl. Phys. Lett. 60 (1992) 1576–1578.
[11] J. E. Graebner, S. Jin, G. W. Kammlott, J. A. Herb, and C. F. Gardinier, Large anisotropic thermal conductivity in synthetic diamond films, Nature 359 (1992) 401–403.
[12] S.L. Shinde, J. Goela, High Thermal Conductivity Materials, Springer, New York, 2006.
[13] K. E. Goodson, O. Kading, and M. Rosler, Experimental investigation of thermal conduction normal to diamond-silicon boundaries, J. Appl. Phys. 77 (1995) 1385–1392.
[14] M. Rabarot, J. Widiez, S. Saada, J. Mazellier, C. Lecouvey, J. Roussin, J. Dechamp, and P. Bergonzo, Silicon-On-Diamond layer integration by wafer bonding technology, Diamond and related materials 19 (2010) 796–805.
[15] E. Bozorg-Grayeli, A. Sood, M. Asheghi, V. Gambin, R. Sandhu, T. I. Feygelson, B. B. Pate, K. Hobart, and K. E. Goodson, Thermal conduction inhomogeneity of nanocrystalline diamond films by dual-side thermoreflectance, Appl. Phys. Lett. 102 (2013) 111907.
[16] F. J. Hernández Guillén, K. Janischowsky, W. Ebert, and E. Kohn, Nanocrystalline diamond films for mechanical applications, Physica Status Solidi (a) 201 (2004) 2553–2557.
[17] M. Necati Ozisik, Heat Transfer: A Basic Approach, Mcgraw-Hill, New York, 1984.
[18] Y. Zhang, P. S. Dobson, and J. M. R. Weaver, High temperature imaging using a thermally compensated cantilever resistive probe for scanning thermal microscopy, Journal of Vacuum Science & Technology B: Microelectronics and Nanometer Structures 30 (2012) 010601.

[19] P. S. Dobson, G. Mills, and J. M. R. Weaver, Microfabricated temperature standard based on Johnson noise measurement for the calibration of micro- and nano-thermometers, Review of Scientific Instruments 76 (2005) 054901.
[20] J.J. Freeman and A.C. Anderson, Thermal conductivity and specific heat of noncrystalline solids, Phys. Rev. B 34 (1986) 5684-5690.
[21] M. Shamsa, S. Ghosh, I. Calizo, V. Ralchenko, A. Popovich, and A. A. Balandin, Thermal conductivity of nitrogenated ultrananocrystalline diamond films, J. Appl. Phys. 103 (2008) 083538.
[22] J. S. Goela, N. E. Brese, M. A. Pickering, and J. E. Graebner, Chemical Vapor Deposited Materials for High Thermal Conductivity Applications, MRS Bulletin 26 (2001) 458–463.
[23] R. T. Bondokov, S. G. Mueller, K. E. Morgan, G. a. Slack, S. Schujman, M. C. Wood, J. a. Smart, and L. J. Schowalter, Large-area AlN substrates for electronic applications: An industrial perspective, Journal of Crystal Growth 310 (2008) 4020–4026.

Table 1: Thickness, lateral grain size and thermal conductivity data for each sample used in this work.

Purpose of study	Sample	Thickness t (nm)	Average in-plane grain size d (nm)	Thermal conductivity k ($Wm^{-1}K^{-1}$)
$\boldsymbol{k_{effective}}$	Set1_a	$t_1 = 370$	77	$k_1 = 230$
	Set1_b	$t_2 = 600$	116	$k_2 = 390$
	Set1_c	$t_3 = 650$	124	$k_3 = 410$
$\boldsymbol{k_{lateral}}$	Set2_a	500	110	276
	Set2_b	1100	188	502
$\boldsymbol{k_{vertical}}$	Set3_a	800	146	~1000

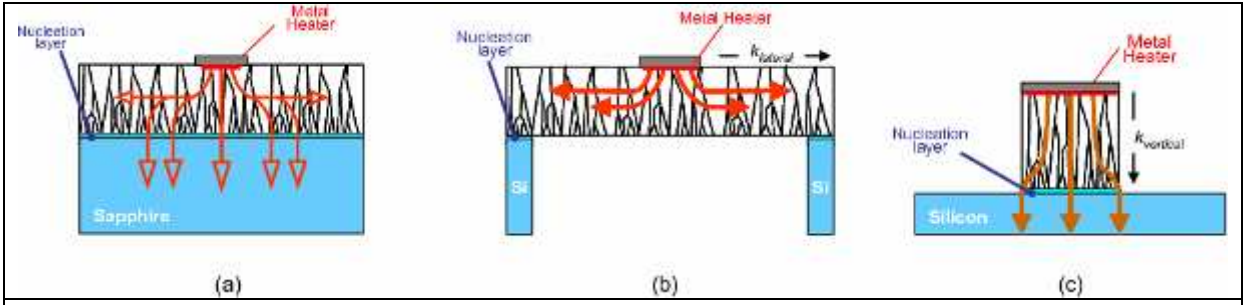

Fig. 1: Test structures for the characterization of NCD thermal conductivity by SThM: (a) structure used to study the thickness dependence of *k*; (b) and (c) structures used to isolate lateral and vertical components of *k* respectively.

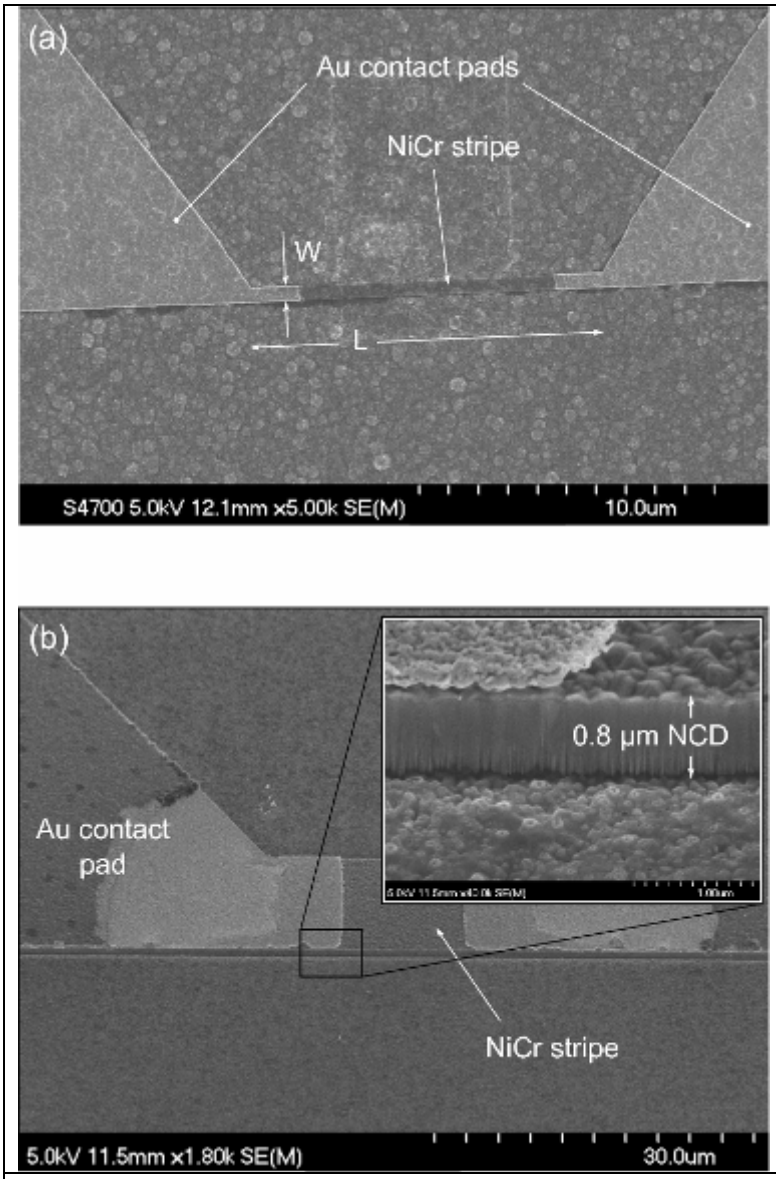

Fig. 2: SEM micrographs of metal heaters fabricated on the NCD surface for (a) Set1 and Set2 and (b) Set3.

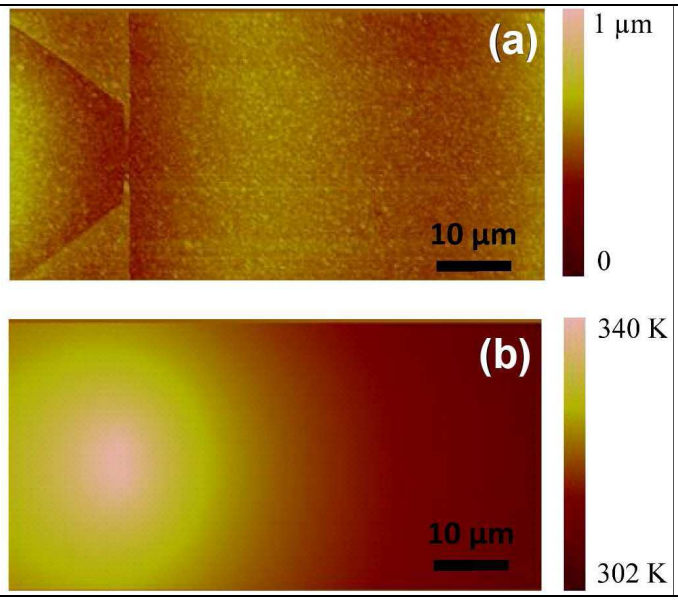

Fig. 3: (a) AFM topographical map and (b) SThM thermal map of the sample surface in the proximity of the metal heater.

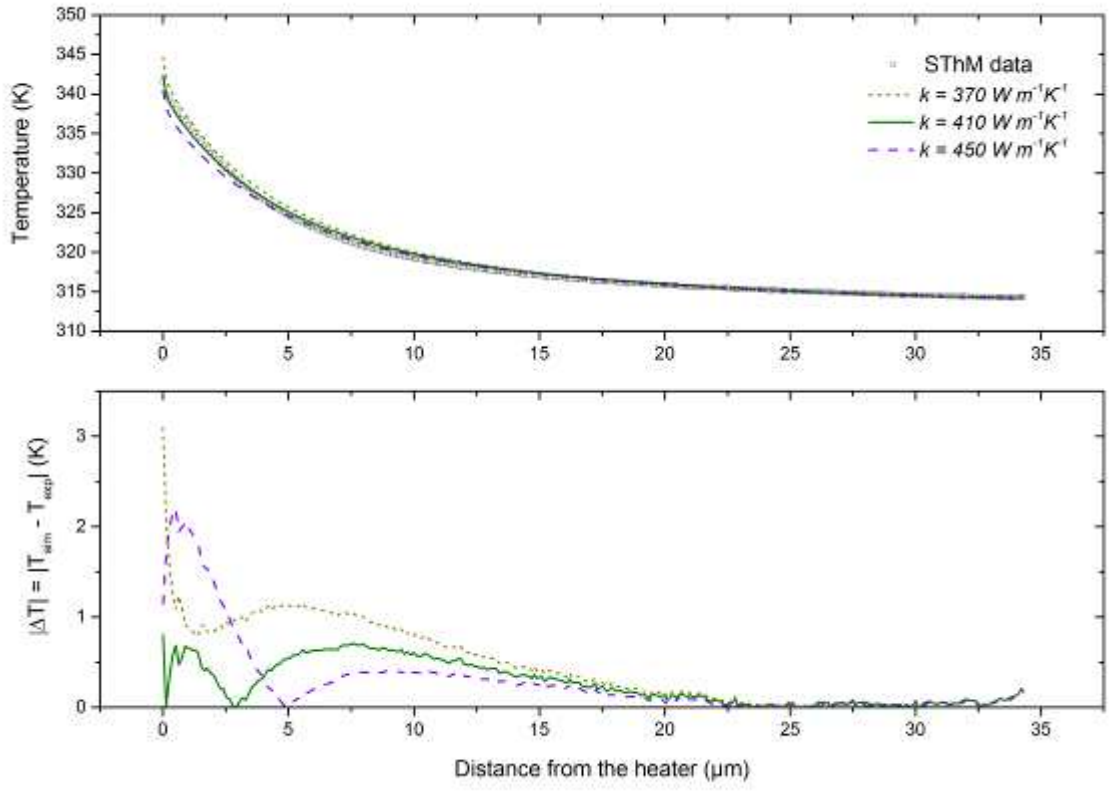

Fig. 4: (a) Right hand side of the temperature profile along the heater centre, fitted by simulated profiles obtained by varying the thermal conductivity of the NCD film in the model. (b) Temperature difference between simulated and experimental data used to identify the best-fit value of *k*.

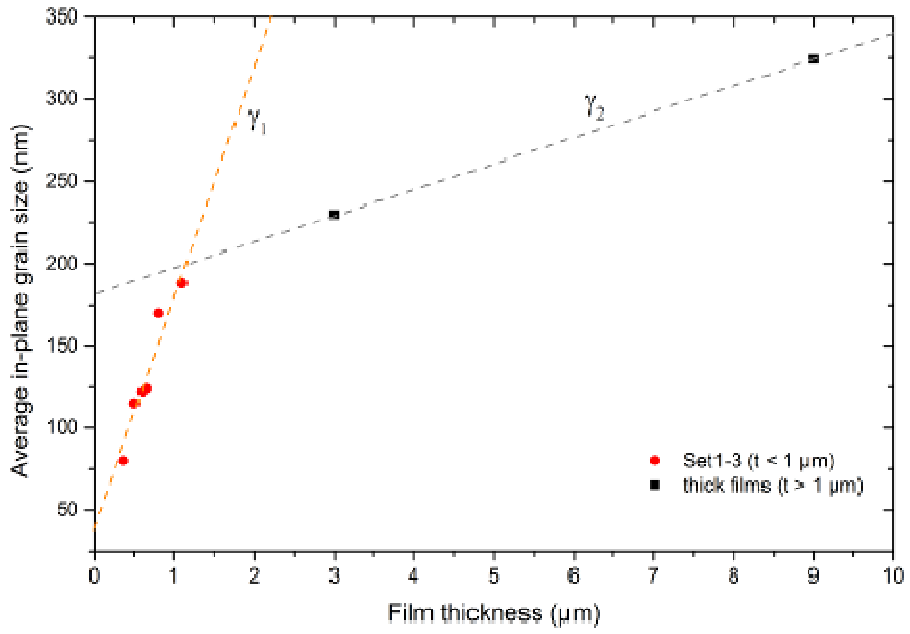

Fig.5: Average in-plane grain size versus film thickness for the columnar-NCD films used in this investigation. The transition from single crystallites to columnar grains takes place in the 1st micron of material, as the change of slope from γ_1 to γ_2 shows. Thick films (■) were not included in the thermal characterization.

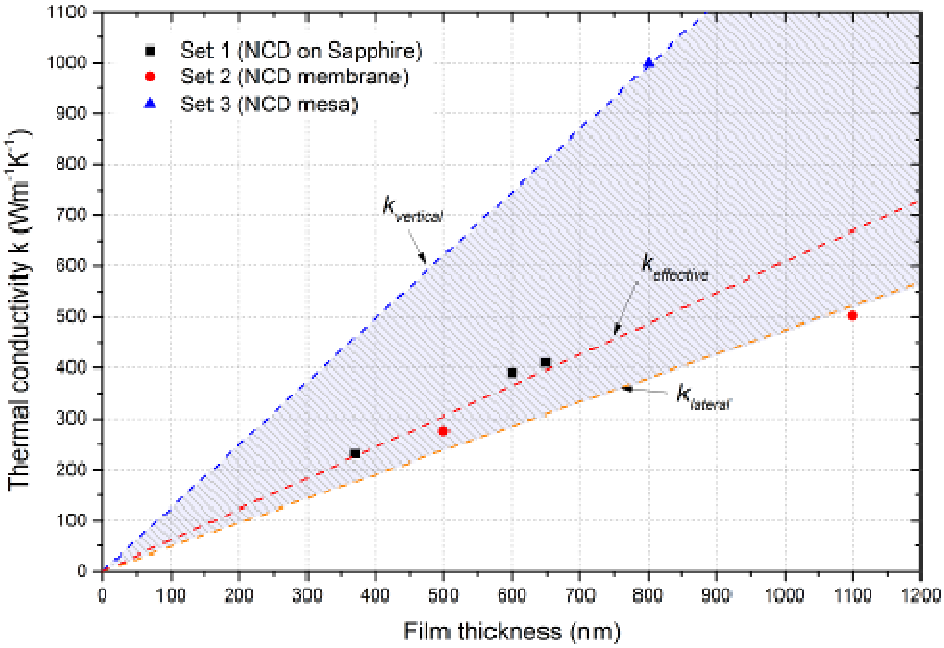

Fig. 6: NCD thermal conductivity values plotted as a function of film thickness for the three set of samples. Trend lines have been drawn according to a linear model. At a fixed thickness, the effective thermal conductivity of the film can vary within the filled area depending on the contribution of lateral and vertical component.